Processing of Nano Carbon Containing Low Carbon MgO-C Refractory : Effect of Mixing Route

Satyananda Behera (satyananda.1990@gmail.com)
IIT BHU: Indian Institute of Technology BHU Varanasi https://orcid.org/0000-0002-7513-3313
Ritwik Sarkar
NIT Rourkela: National Institute of Technology Rourkela

Research Article

Keywords: nanocarbon, MgO-C refractory, mixing, processing, microstructure

Posted Date: September 28th, 2020

DOI: https://doi.org/10.21203/rs.3.rs-82745/v1

Abstract

Nano carbon, being finer in size, is difficult to mix uniformly in a refractory composition to achieve the advantages of nano-metric size and its associated properties. Development of N220 nano carbon containing MgO-C refractory has been studied by using three different mixing and processing routes. The developed products of different processing routes are compared by evaluation of the developed properties against the conventional 16 wt% graphite containing commercial MgO-C refractory composition. Nano carbon containing composition with optimized processing route is further characterized for phase analysis; microstructural studies; elemental distribution of carbon; thermal shock resistance, and pore size distribution and also compared against the conventional composition. batch prepared by the optimum processing route were further studied for measured by oil bath quenching method and thermal cycle method.

1.1 Introduction

Magnesia carbon (MgO-C) refractories are widely used in iron and steel industries due to excellent corrosion and thermal shock resistances, coming mainly from the presence of graphite, having high thermal conductivity and low wetting properties with high refractoriness. Generally MgO-C refractories contain about 12–18% total carbon and the primary source of carbon is graphite [1-4]. Use of graphite as carbon source offers the following major advantages to the refractory.

- Higher application temperature due to high melting point and no eutectic formation.
- Improvement in the corrosion resistance against metal and slag due to very low wettability.
- Increase in thermal conductivity, reduction in thermal expansion and elastic modulus, resulting in excellent thermal shock resistance.
- Better packing efficiency due to lubrication property
- Reduced chances of iron oxide corrosion as iron oxide may reduce to metallic Fe by C.

These advantages, due to incorporation of carbon (as graphite) have initially attracted the refractory manufacturers to use more and more amount of carbon, but as the time progresses, knowledge and technological developments have made it clear that higher carbon content in the refractory also imparts several drawbacks too, like, [5-7]

- Greater extent of oxidation results in highly porous poorly bonded weak refractory that is easily penetrated and corroded by slag.
- Increased thermal conductivity of refractory increases the energy loss through the wall, increasing the specific energy requirement per unit of steel produced.
- Increased heat transfer to outer wall increases the shell temperature, resulting in damage and deformation of metallic shell.
- Increased chances of carbon pick-up by molten metal.

- Generation of higher extent of CO_x

To overcome the drawbacks, in the recent years, a number of researchers have studied and developed MgO-C material with excellent physical properties through the addition of nanometer carbon black in order to improve the structure of binding carbon. Nano carbons absorb and relieve the stress due to thermal expansion and shrinkage of refractories and also reduce the mal-distribution of thermal stress in the inner portion of refractories, resulting in improvement in thermal shock resistance properties [8].Magnesia carbon bricks with nano structured matrix were developed using hybridized graphite black (HGB), synthesized from carbon black and boron through the induction field activated SHS (Self–propagating High-temperature Synthesis)method, were found to have outstanding features i.e. excellent resistances against thermal shock, corrosion and oxidation, led to durability and were applied to RH degassers with very high success rate [9].

Nanomaterials are finding their way into an increasing number of modern products. Manufacturers and users of nano-materials get benefit on introduction of small amounts of nanomaterials into their products as that improves existing properties havoc or provide new functionalities. This trend does come with a new set of unique processing challenges, however, including the efficient mixing and dispersion of nanoparticles into a formulation. Next generation of high performance structural materials and coatings are believed to routinely employ nanoparticles and nanocomposites due to their attractive qualities like excellent wear and corrosion resistances, strength and hardness. The unique properties of nanoparticles arise from their size reduction. When a particle is reduced down to the nanosize range (usually defined as 1–100 nm), a much larger surface area per unit volume is achieved, and even more importantly, a dramatically increased percentage of molecules or atoms are found to be present on its surface. At the point where the interaction length scales of physical, mechanical and thermos mechanical phenomena become comparable to the size of the particle, crystal or grain structure, new properties and phenomena emerge.

Furthermore, when nano-particles are used to make a composite, a combination of improved properties can be obtained, which is not available in any conventional composite, since at nano-scale, material properties are strongly influenced by atomic or molecular interactions. Since the building blocks of a nanocomposite are of nanoscale, many interfaces exist between the two intermixed solid phases and the special properties of a nanocomposite arise from phase interactions at these interfaces Thus, the ability to prepare well-mixed nanocomposites is extremely important.

In this article different mixing routes were used for the processing of MgO-C refractories by incorporating nano carbon black partially replacing graphite content and grossly reducing the total carbon content. Further various refractory related properties of the developed products were evaluated.The samples were coked in a reducing environment at 1000^0C for 4 hours and the matrix phase of the composites were studied through FESEM and XRD for the understanding of phase formation and micrographs.

2.1 Experimental

Commercially available high purity fused magnesia (Chinese source, supplied by Magus Marketing, India) of sizes 3-1 mm, 1-0.075 mm and <75 micron, natural flake graphite (Agarwal Graphite Industries, India) and N 220 nano carbon black (Birla carbon, India) were used as starting materials. Resol type of phenolic formaldehyde resin were used as binder and aluminum metal powder (98% pure and finer than 100 micron) and boron carbide powder (95% pure, total B = 77 wt%, total C = 21 wt% and size < 150 micron) were used as anti-oxidant in this process.Physico-chemical properties of the raw materials show (table 1A-C) that fused magnesia is >97% pure with CaO as the main impurity. Graphite is also > 94% pure and has ash content as the main impurity. N 220 nano carbon black is also very high pure and very fine, having specific surface area > 120 $m^2.g^{-1}$. The details of batch compositions studied are given in table 2. Batches were planned to study conventional MgO-C composition with 16 wt% graphite and two other 1 wt% nano-carbon containing low carbon MgO-C refractory, as per previous works [10-13]. All the batches were processed in there different routes. The flow diagramdetails of the three different batch mixing processesare given in Fig 1-3. In route one, the nano carbon was added with coarse magnesia grains whereas nano carbon was added with other fines in route two and three. After mixing all the batches processed in different mixing sequences were pressed at 150 MPa in a hydraulic uni-axial press and then cured at 220^0C For 12 hours. Nano carbon containing optimized batch and the conventional batch were further evaluated for microstructural and phase analysis study after coking. The sampleswere coked in reducing atmosphere at 1000^0C for 4 h in an alumina crucible closed with a lid. Cureddensity and cold crushing strength (CCS) of cured samples were measured as per the standard of IS: 1528, Part-12 (2002) and IS: 1528, Part-4 (2002) respectively. The microstructure and phase analysis studies were evaluated for the optimized batch. Elemental distribution of carbon was also studied by using EDAX attachment with the FESEM (FEI, US make) for the conventional batch and optimized batch processed through the optimized route. The thermal shock resistance was determined, for the optimized batch and conventional batch processed through the optimized route,by standard air quench method in which the sample (50 mm dia and 50 mm height) was at 1400ºC for 10 minutes in a raising hearth furnace (Bysakh India make) and cooled subsequently to room temperature. Thenumber of thermal cycles that the sample can withstand till failure (crack formation) was measured. Simultaneously the thermal shock resistance of the specimens fired at 1400 °C was measured by oil bath quenching method. The specimens were heated in a coke bed up to 1100 °C with a heating rate of 5 °C/min, and soaked at this temperature for 10 min. Then, the specimens were taken out and quickly quenched in an oil bath. The purpose of using oil bath instead of the water bath was to prevent oxidation and hydration of the specimens. After completion of each cycle, upto 3rd cycle, the strength was measured. Mercury intrusion porosimetry (Micromeritics, US make) was studied for the optimized batch and conventional batch processed through the optimized route. Mercury was intruded in the pores of the sample by increasing the pressure on the mercury, and the pore sizes are calculated as per Young-Laplace or Washburn equation

$\Delta P = \gamma\ (1/r_1 + 1/r_2) = 2\gamma Cos\theta\ /\ r$ ……..(4.3)

Where r = radius of the Capillary Pore, γ = liquid-vapor interfacial tension, θ = contact angle between the liquid and capillary wall. Pore size distribution of the samples were evaluated by plotting the incremental

intrusion volume of mercury against pressure / pore size.

3.1 Result And Discussion

3.1.1 Density

The density values in gm/cc of all the batches processed through there different routes are shown in figure 4. In each route,the conventional batch i.e 16 wt% graphite containing batch, shows a less density values compared to the nano carbon containing batch because of greater extent of magnesia (higher density) present and better filling of the void spaces among the magnesia grainsby much finer nano carbon particles(10-13). Comparing the three different mixing routes for the processing of the batches, route 1 has shown better density values than other two routes. This is mainly due to better mixing of nano carbon in magnesia when it is in mechanical stirring in dry and hot condition with coarser MgO fraction. So, the dispersion of the nano carbon is better and the magnesia grains are well coated with the fine nano carbon through route 1. In other routes, the nano carbon was added with all the other fine particles, thus coating of nano carbon was not that effectiveresulting in poorer density comparable to route.

3.1.2 Strength

The variation of cold crushing strength (CCS) of all the cured batches, with the variation in the mixing route, is shown figure 5. The strength of the nano carbon containing batches are higher compared to that of the conventional batch is due to greater filling of the void spaces by much finer nano carbon particles compared to that of graphite particles, resulting in better compaction. In Route 1, the strengthof all the compositions show greater values compared to the other two routes. This is because of the well dispersion of nano carbon in the refractory composites and able to fill the tinypores among the magnesia grains. But in the other routes, nano carbon is added with all other fine particles which may not be dispersed uniformly in the refractory matrix due to the agglomeration tendency of fines components (higher surface area).

3.1.3 Microstructure and phase analysis study

The microstructural and phase analysis study of batch no 3processed through route 1 are shown in Fig 6 and 7 respectively. The detailed phase and microstructural analysis were done for the same composition in a previous study (13). Formation and well distribution of rod type Al_4C_3 and spinel phases are confirmed by x-ray diffraction as well as microstructural study (14-16). Higher reactivity of much finer nano carbon particles and their well distribution during mixing with the magnesia grain resulting in greater extent of formation of insitu ceramic phase like spinel and aluminium carbide(fig 7)

3.1.4 Thermal shock resistance

The Thermal shock resistance of the optimized batch 3 was studied and compared against batch composition 1, prepared by the process Route 1. Fig 8 shows the strength retainment (as CCS) capacity of the batches after different numbers of thermal cycles. It has been observed that there is an increase in strength values upto 2nd cycle. This increase in strength may be due to the formation of micro cracksin the both samples. Formation of spinel due to the reaction between alumina (forming on oxidation of aluminium metal powder) and fine magnesia in the matrix phase results in the creation of micro cracks due to the thermal expansion coefficient mismatch with magnesia. This thermal expansion mismatch has occurred during the initial thermal cycles causing the formation of micro cracks within the matrix. On further thermal shocks, these micro cracks also grow due to greater extent of thermal strain produced during increase cycles and resultin the propagation of cracks. Thus causing failure of the samples at a much lower strength retention capacit values..

This spinel formation is common on the both the batch 1 and batch 3, however low carbon containing composition produces higher extent of spinel due to the higher reactivity of nano carbon and greater formation of aluminium carbide which oxidized to form reacting alumina and hence produces more amount of spinel in the composition [13]. So the effect of micro cracking is higher in nano carbon containing composition and strength retention capacity is also higher.

But further increasing thermal shock cycles, this micro cracking effect is not very strong, and the strength retention capacity sharply decreases with increasing number of thermal cycles.

Fig 9 represents the number of thermal shock cycles that these batches can withstand. Cracks were observed only after 14 and 15 cycles for the nano carbon containing (batch 3) and conventional (batch 1) compositionsrespectively. However, after 12 cycles, the conventional composition showed a diskuling/peeling off effect on its surface where a layer of refractory was peeled off and detached without creating/formation of any visible cracks. As there was no crack, thermal shock test was continued for the sample. This peeled off effect of the skin was observed after 12ththermal cycle without any crack formation. However no such effect was observed for the nano carbon containing composition. The crackwas first observed in nano carbon containing composition at its 15thccle and for conventional composition 16thcycle. There is hardly any difference observed in this two compositions.

3.1.5 Distribution of carbon and matrix phase

Photomicrographsof the cured samples of batche 1 and 3, processed through route 1, are shown in Fig 10 A and B respectively. Here, it is clearly visible that in batch 3, the magnesia grains are well coated with the matrix phase containing nano carbon,whereas in batch 1, the coating was not proper. Thus the effect and advantages of presence of carbon is better for batch 3.

Elemental distribution of carbon for batch 1 and 3 are studied using scanning electron microscope and shown in fig 11. Uniform distribution of carbon particles was observed (as white spots), and no agglomeration was found in both the batches. The figures show that carbon is well distributed all through the body even at low carbon content. Uniform distribution of nano carbon black particles has resulted in

to achieve similar of better properties even at much lower carbon content, compared to that of conventional composition.

3.1.6 Pore size distribution

The pore size distribution by mercury intrusion for the batch 1 and batch 3 prepared through route 1 are shown in fig 12 and 13 respectively. Mercury intrusion porosimetry data shows (fig 12) that pores are present in two major size clusters for the conventional batch 1. The coarsest one is in the size range of ~ 250 to 60microns and the second one in the range of ~ 1 to 8 microns. These two different discrete size ranges of pores may be due to the presence of voids amongst coarse and medium particles and also between the medium and fine particles and among the fine particles in the composition. Pores present in the submicrometer or nanometer size ranges ae found to be negligible. The size of the pores and its volume fraction, especially the coarser one, is big enough to affect the strength and corrosion and penetration properties. The presence of graphite, even at 16 wt% is not good enough to fill the pores and minimize the size and fraction. Thus the conventional composition is found to have relatively lower refractory properties.

On the other hand, batch 3 shows reduced extent of porosities in these pore size ranges. This is mainly due to the filling of the pores in both the size ranges by much finer nano carbon particles, resulting in reduced volume of pores, thus enhancing compaction of the composition and resulting in improved properties. Also, a great reduction in pore volume in the range of ~ 1 to 10 micron size indicates that the nano carbon particles are in well dispersed (not in agglomerated) form and thus fill the finer size fraction of the pores. But, in the presence of nano carbon, a new type of pores, in the range of 20 to 30 nano meter, is observed. Such a finer size of pores is formed may be due to the inter-particle porosity present among the nano carbon particles. However, the size range of these new pores is such small that they will not adversely affect the strength and corrosion properties of the compositions.

Conclusion

Different compositions of MgO-C refractory were prepared by three different mixing routes to optimize the process route for mixing nano carbon in the refractory composition. The density and strength values of 1 wt% N220 nano carbon containing batch was found to be optimum and the process route wherein the nano carbon was mixed with the coarse fraction of MgO in dry condition was found to be the best one.Formation of aluminum carbide and magnesium aluminate spinel phases was found in the N220 nano carbon containing low carbon batch. Nano carbon containing composition prepared through the optimized route showed uniform distribution of carbon in elemental mapping study, comparable or better thermal shock resistance property and much reduced and finer pore size distribution indicating much improved properties compared to that of the conventional 16 wt% graphite containing batch.

Declarations

Acknowledgement

The authors thankfully acknowledge the support of all the technical staffs of Department of Ceramic Engg, NIT, Rourkela and the financial support of the TSD group of DST for supporting the work as sponsored research project (DST/TSG/ Ceramic/2011/143).

Reference

[1] Barthel, H. Effect of carbon in tar-impregnated burnt magnesite bricks on the wear of basic oxygen furnace linings. [J] Stahl u. Eisen. 1966, 86, 81–88.

[2] Limes, R.W. Refractories for basic oxygen furnace. J. Met. 1966, 18 (17) 865– 869.

[3] Herron, R.H; Beechan, C.R; Padfield R.C. Slag attack on carbon bearing basic refractories. Amer. Ceram. Soc. Bull. 1967, 46 1163–1168.

[4] Pickering, G.D; Batchelor, J.D. Carbon-MgO reactions in BOF refractories. Amer. Ceram. Soc. Bull. 1971, 50 611–614.

[5] Bag, M; Adak, S; Sarkar, R. Study on low carbon containing MgO-C refractory: Use of nano carbon. Ceram. Int., 2012, 38, 2339–2346.

[6] Peng, S; LI, L; Peng, D. The progress of low-carbon MgO–C composite study, Refractories. 2003, 37, (6), 355–357.

[7] Boquan, Z; Wenjie, Z; Yashuang, Y. Current situation and development of low-carbon magnesia–carbon materials research, Refractories. 2006, 40, (1), 90–95.

[8] Ochiai, T. The development of refractories by applying nano-technology. Refractories, 2004, 56, (4), 152–159.

[9] Matsui, T; Goto, T; Yamada, Y; Taki, N. Characteristics and applications of nano tech magnesia carbon bricks, in: Proceedings of the 9th UNITECR- 2005, November 8–11, Orlando, FL, USA, 2005.

[10] Behera, S; Sarkar, R. Low-Carbon Magnesia-Carbon Refractory: Use of N220 Nanocarbon Black, Int. J. Appl. Ceram. Technol. 2014, 11, [6], 968–976.

[11] Behera, S; Sarkar, R. Study on the variation of graphite content in N220 nano carbon containing low carbon MgO-C refractory. J of Ironmaking and Steelmaking. 2016, 43, [2], 130-136.

[12] Behera, S; Sarkar, R. Nano Carbon Containing Low Carbon Magnesia Carbon Refractory: an Overview. Prot of Met and Phy Chem of Surfaces, 2016, 52, [3], 467–474.

[13] Behera, S; Sarkar, R., Effect of different metal powder anti-oxidants on N220 nano carbon containing low carbon MgO-C refractory: An in-depth investigation. Cera Int. 2016, 42, [16], 18484-18494.

[14] Das, R. R.; Nayak, B. B.; Adak, S.; Chattopadhyay, A. K. Influence of nanocrystalline MgAl2O4 spinel addition on the properties of MgO-C refractories. Mat. and Man. Proc. 2012, 27, (3), 242-246.

[15] Yang, L.; Xiao, G.; Ding, D.; Li, P.; hua Lv, L.; lei Yang, S. Soild-phase synthesis of MgAl 2 O 4 powder in reducing atmosphere: Effects of alumina sources and addition of carbon black. Mat. Res. Expr. In press, DOI: https://doi.org/10.1088/2053-1591/aaf967

[16] Liu, Z.; Yuan, L.; Yu, J. Improvements in the mechanical properties and oxidation resistance of MgO-C refractories with the addition of nano-Y2O3 powder. Adv. in App. Ceram, 2019, DOI; https://doi.org/10.1080/17436753.2018.1564414.

Tables

Table 1: Physiochemical properties of the raw materials.

A. Fused Magnesia:

Raw Materials	MgO	Al_2O_3	SiO_2	CaO	Fe_2O_3	Na_2O
Fused Magnesia	97.35	0.07	0.40	1.40	0.22	0.26

B. Flaky Graphite:

Raw Materials	Carbon (%)	Volatile Matter (%)	Ash (%)	Surface area (m^2g^{-1})
Flake Graphite	94.1	0.80	5.08	5.7

C. Nano Carbon Black (N220):

Raw Materials	Carbon (%)	Volatile Matter (%)	Ash (%)	Surface area (m^2g^{-1})
Nano carbon black (N220)	98.29	1.3	0.19	120.1

Table 2: Batch Composition

Component	Batch 1	Batch 2	Batch 3
Fused MgO	80	90	91
Graphite	16	5	3
Al metal powder	2	2	2
Boron carbide	1	1	1
Carbores P	1	1	1
N 220Nano carbon	0	1	2
Powder resin	2	2	2
Liquid resin	3.5	3.5	3.5

Figures

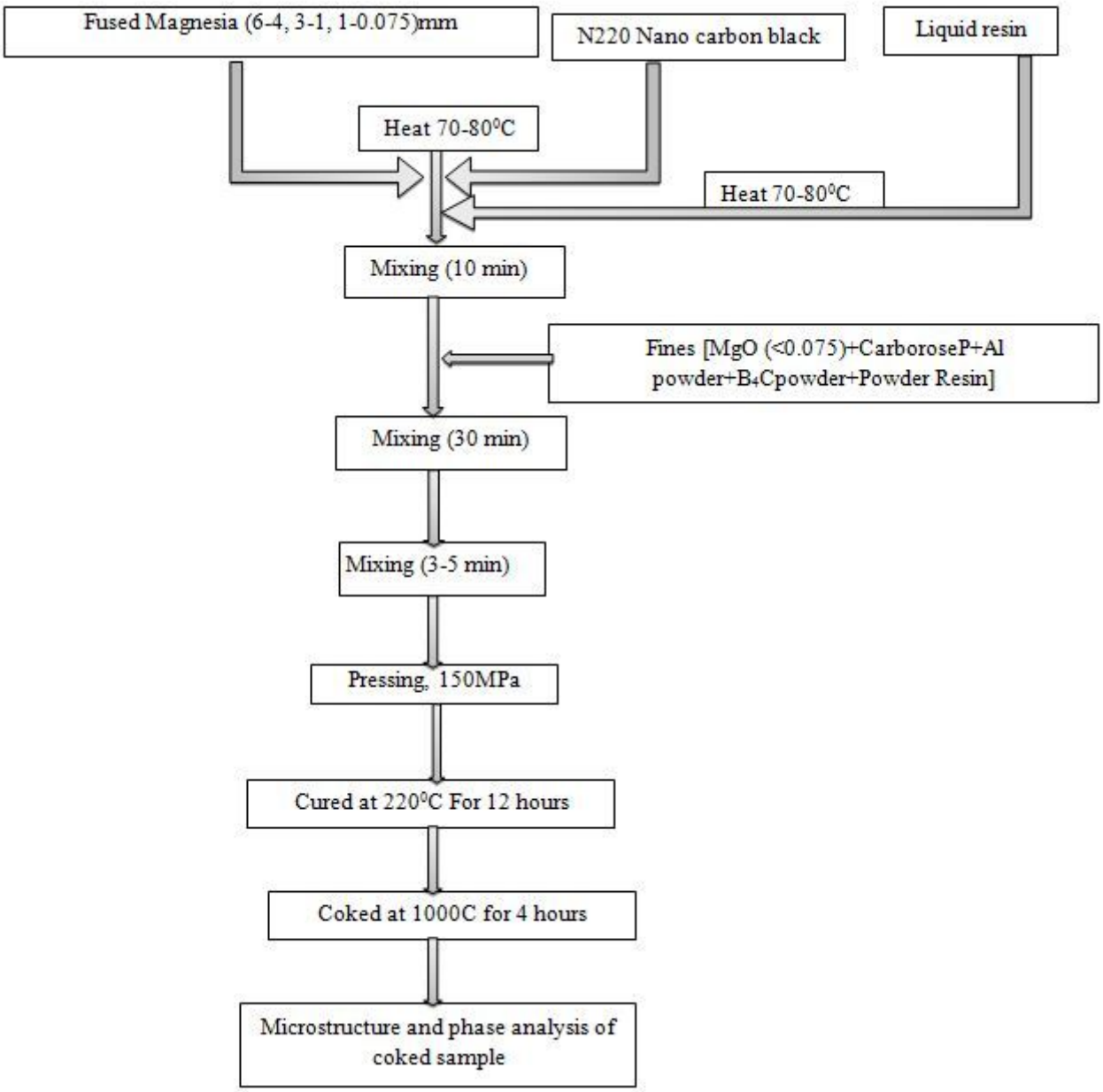

Figure 1

Flow diagram of Route 1 mixing

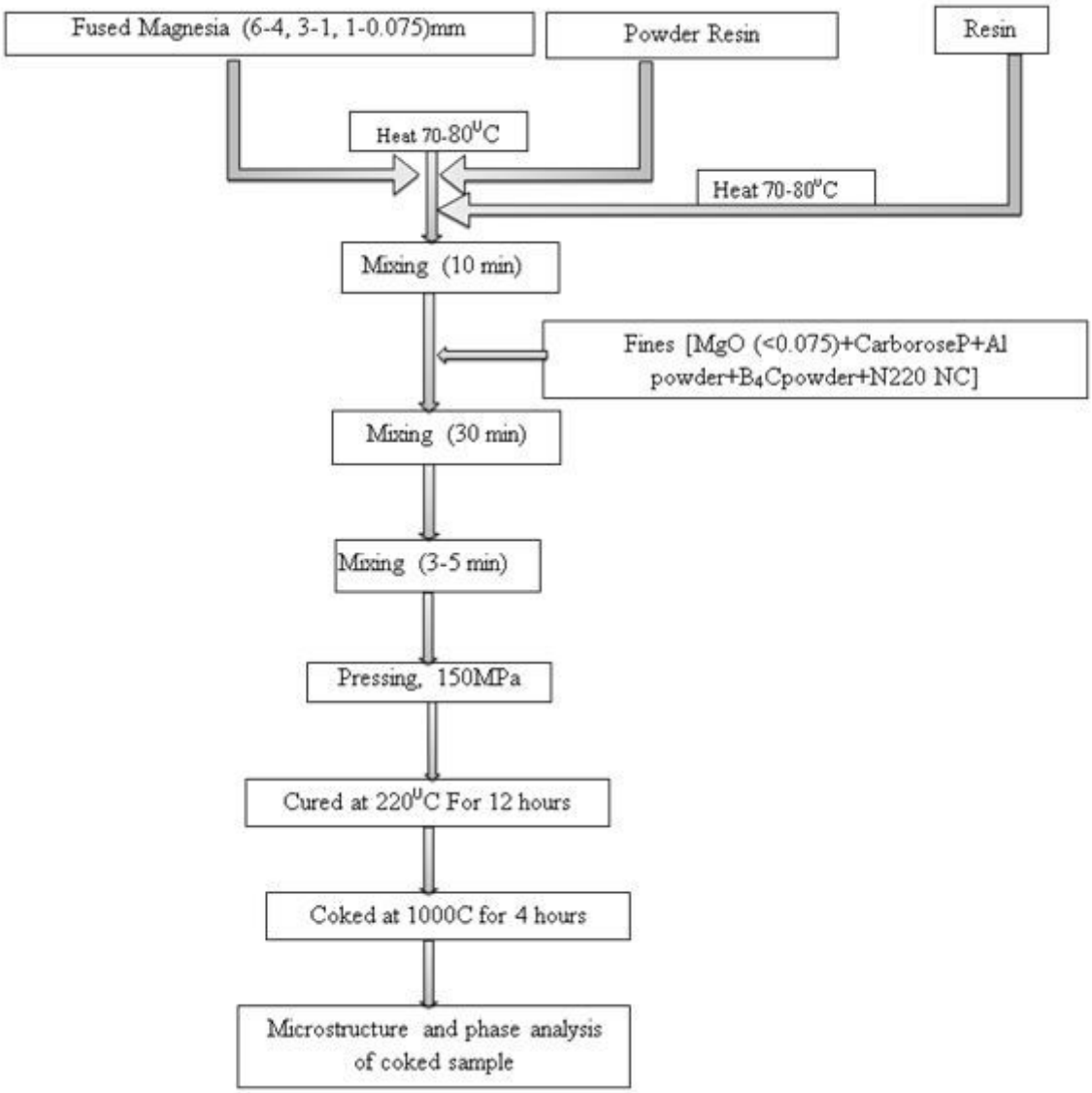

Figure 2

Flow diagram of Route 2 mixing

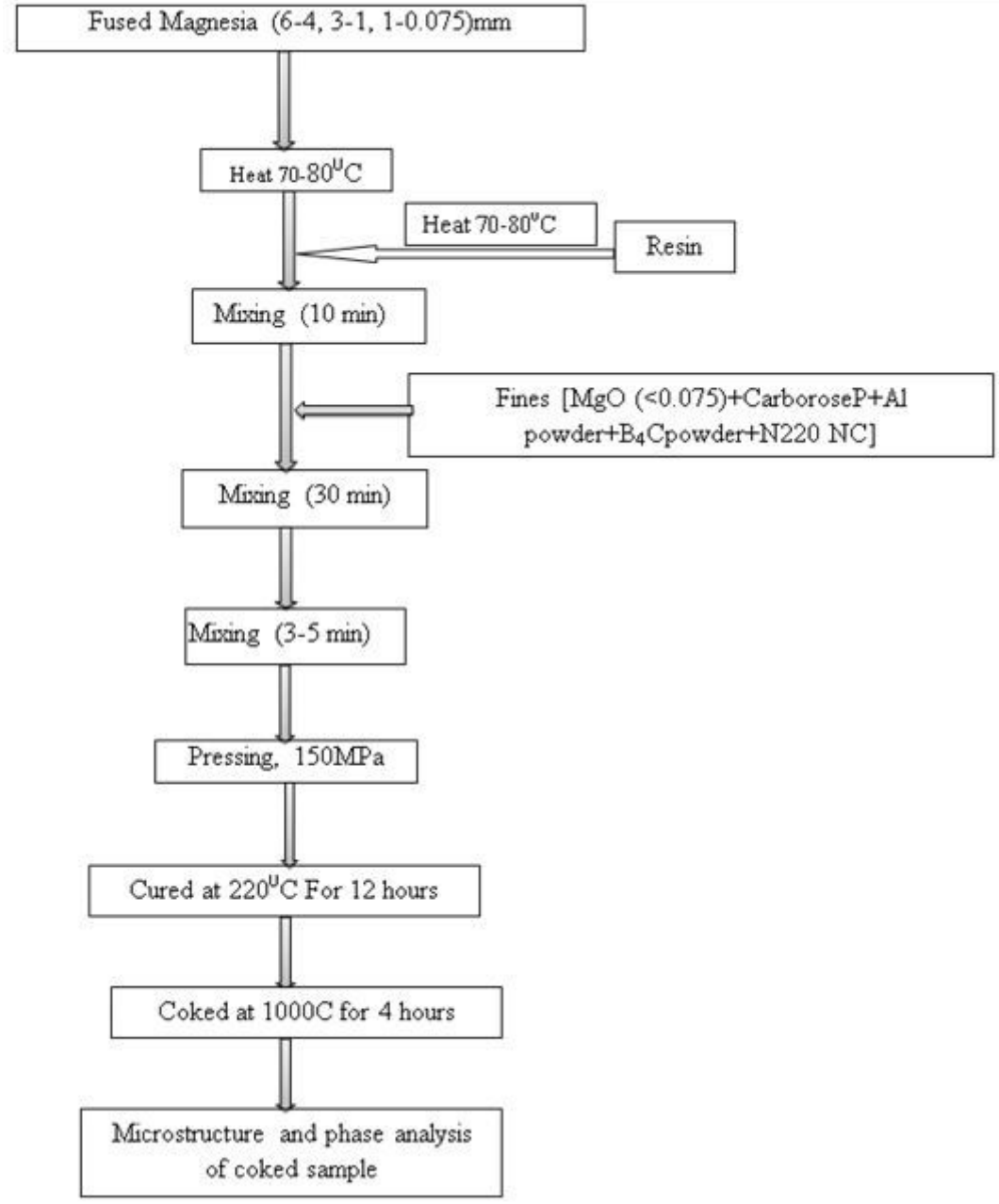

Figure 3

Flow diagram of Route 3 mixing

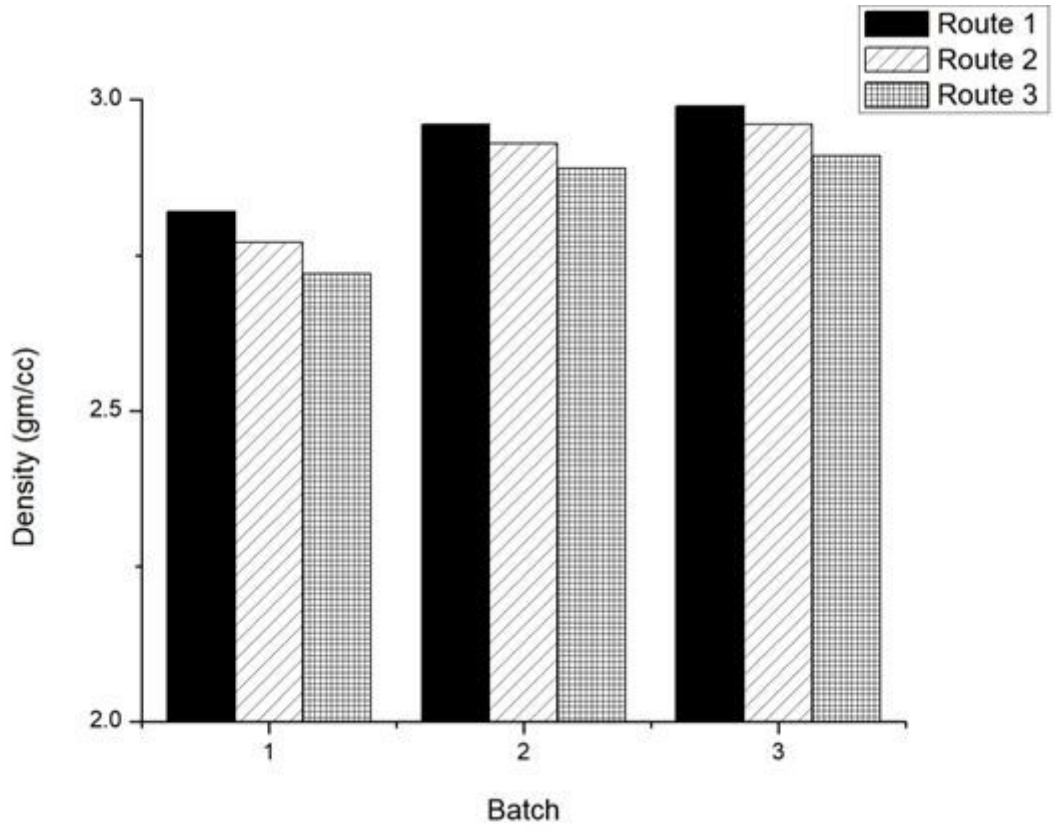

Figure 4

Bulk density values of different batches prepared through different mixing routes

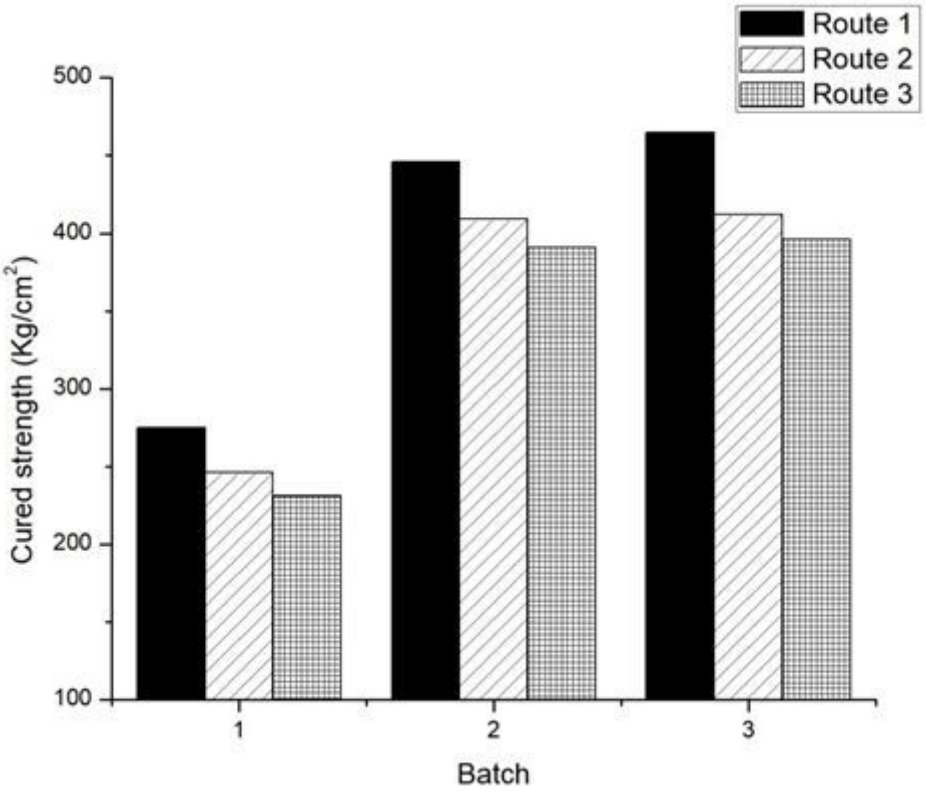

Figure 5

Cured strength of different batches prepared through different mixing routes

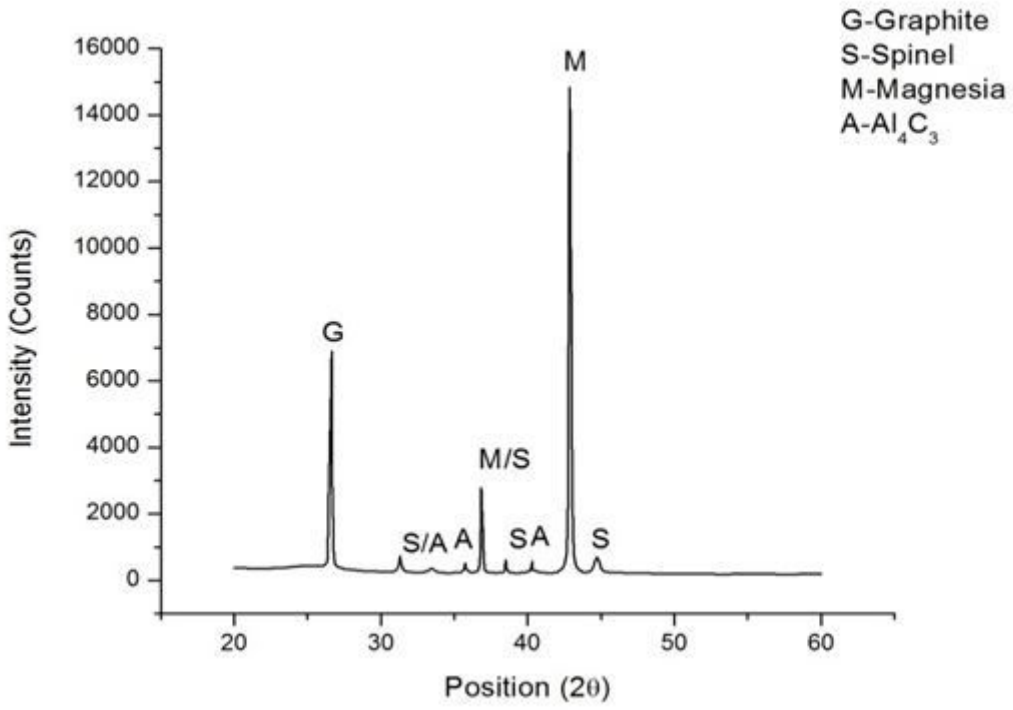

Figure 6

Phase analysis study of batch 3 processed through mixing route 1.

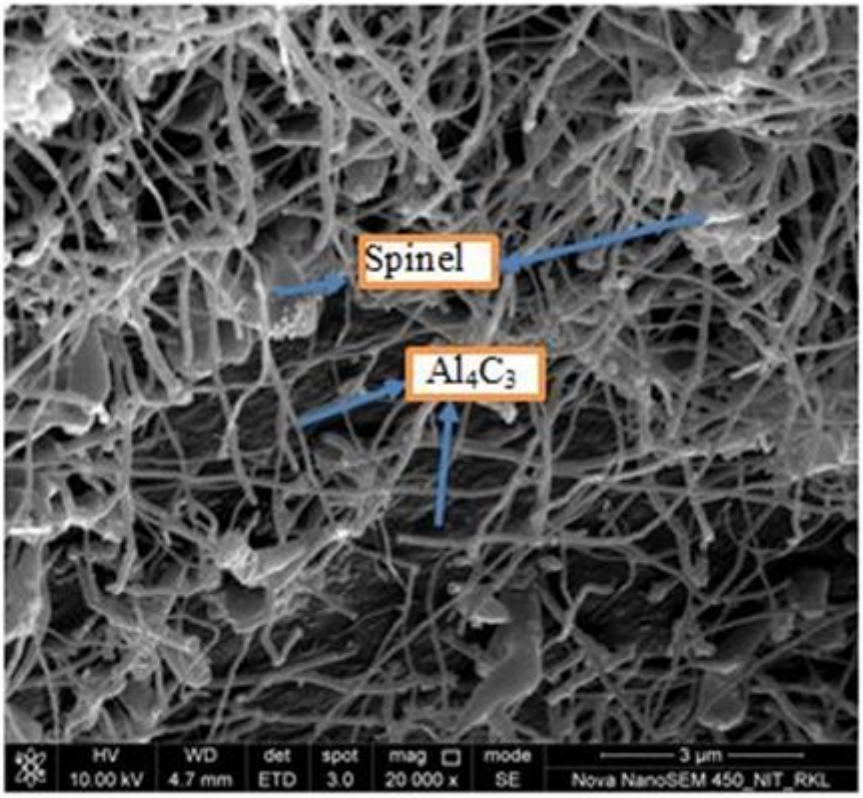

Figure 7

Microstructural study of batch 3 processed through mixing route 1.

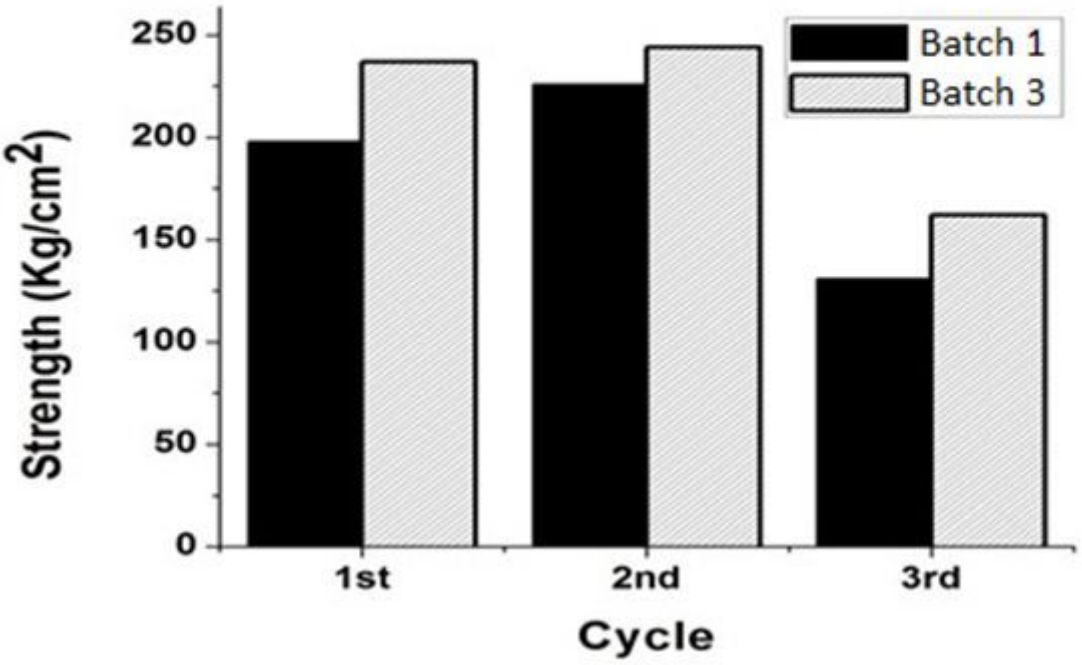

Figure 8

Strength retainmentcapacity of the batches after thermal cycles.

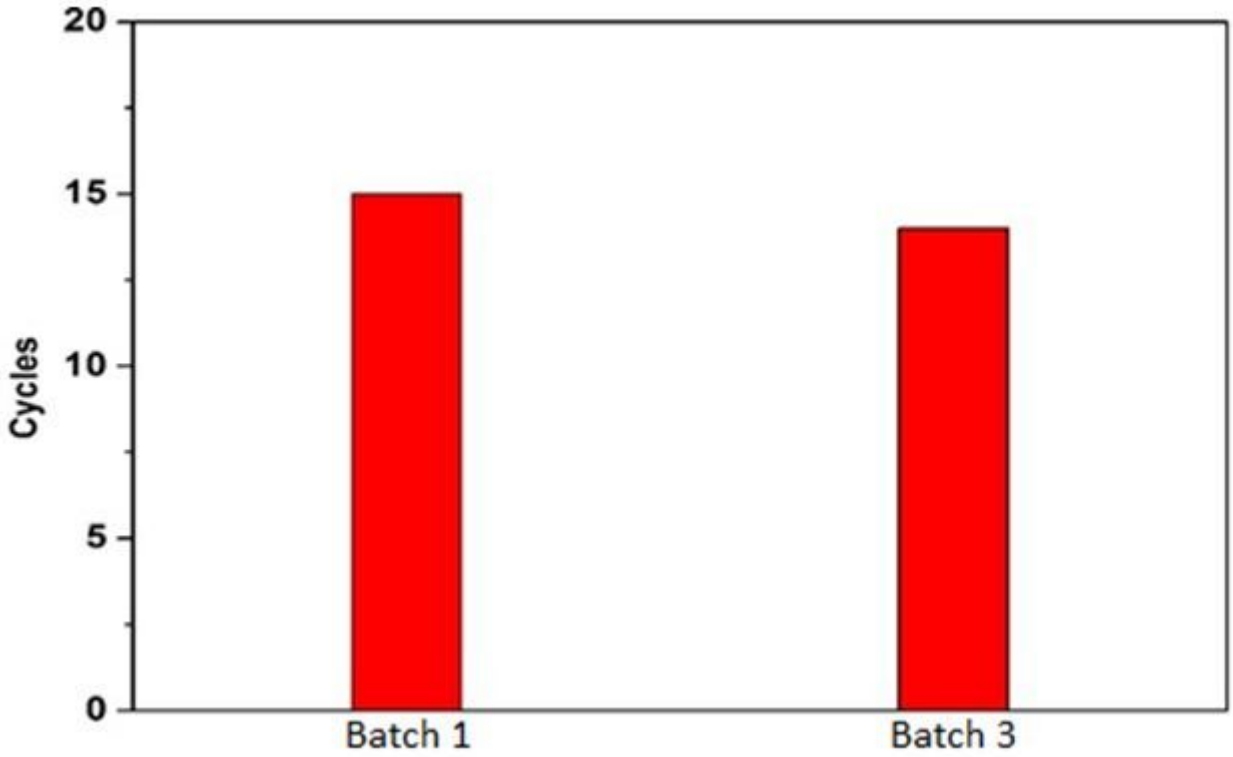

Figure 9

Thermal shock resistance of the batches measured by number of thermal cycles

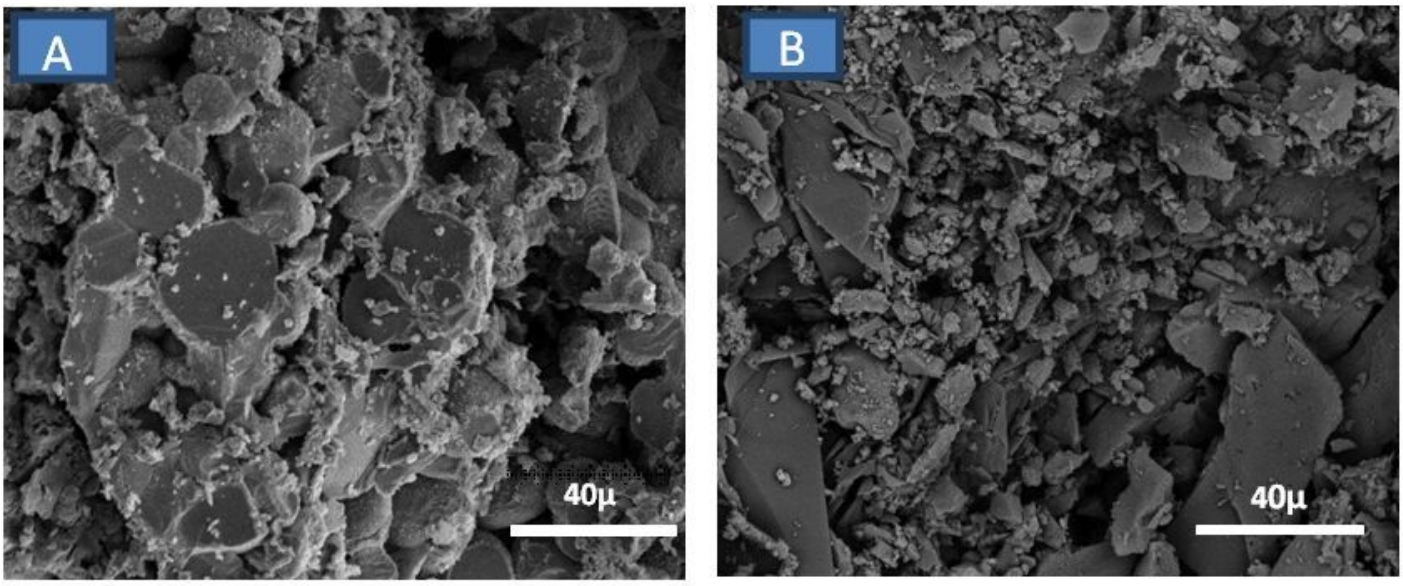

Figure 10

Matrix phase distribution in cured samples of batch 3 (A) and batch 1 (B) prepared by route 1

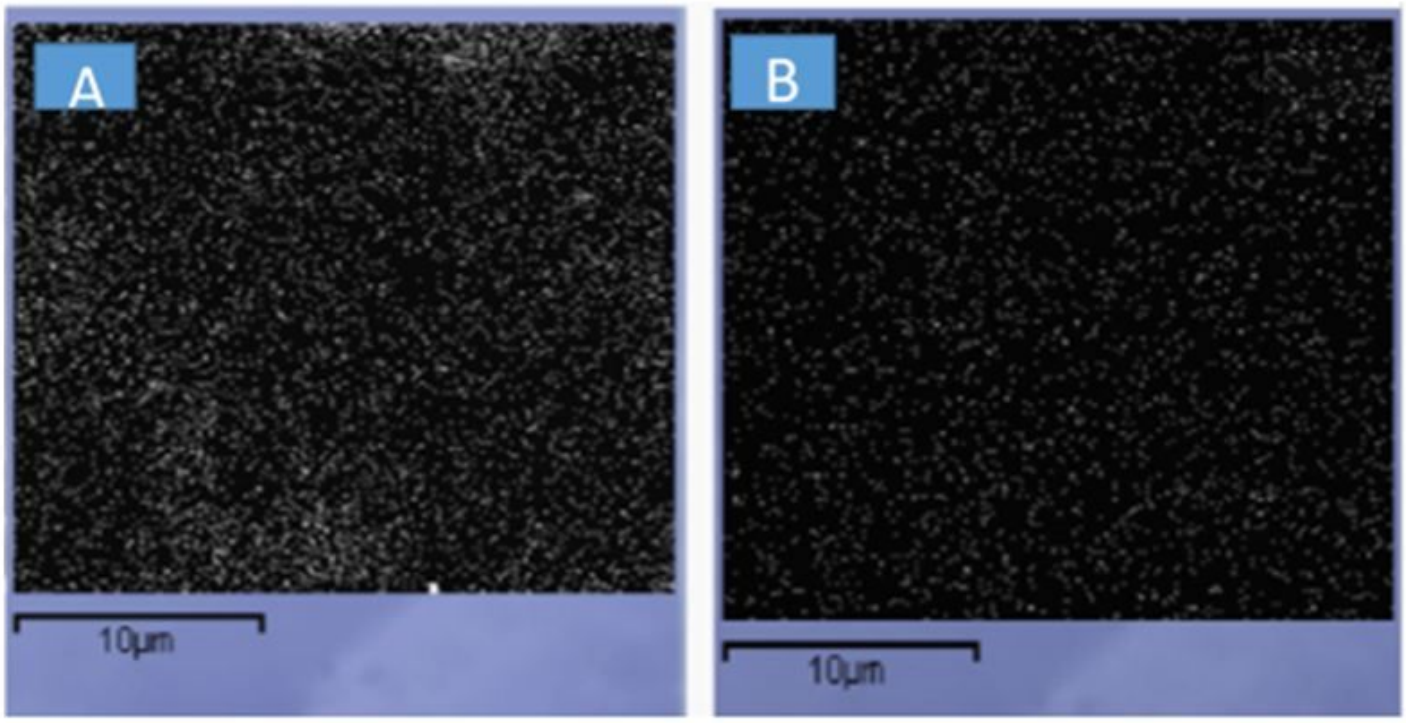

Figure 11

Elemental carbon distribution in the matrix phase in batch 1 (A) and batch 3 prepared through route 1.

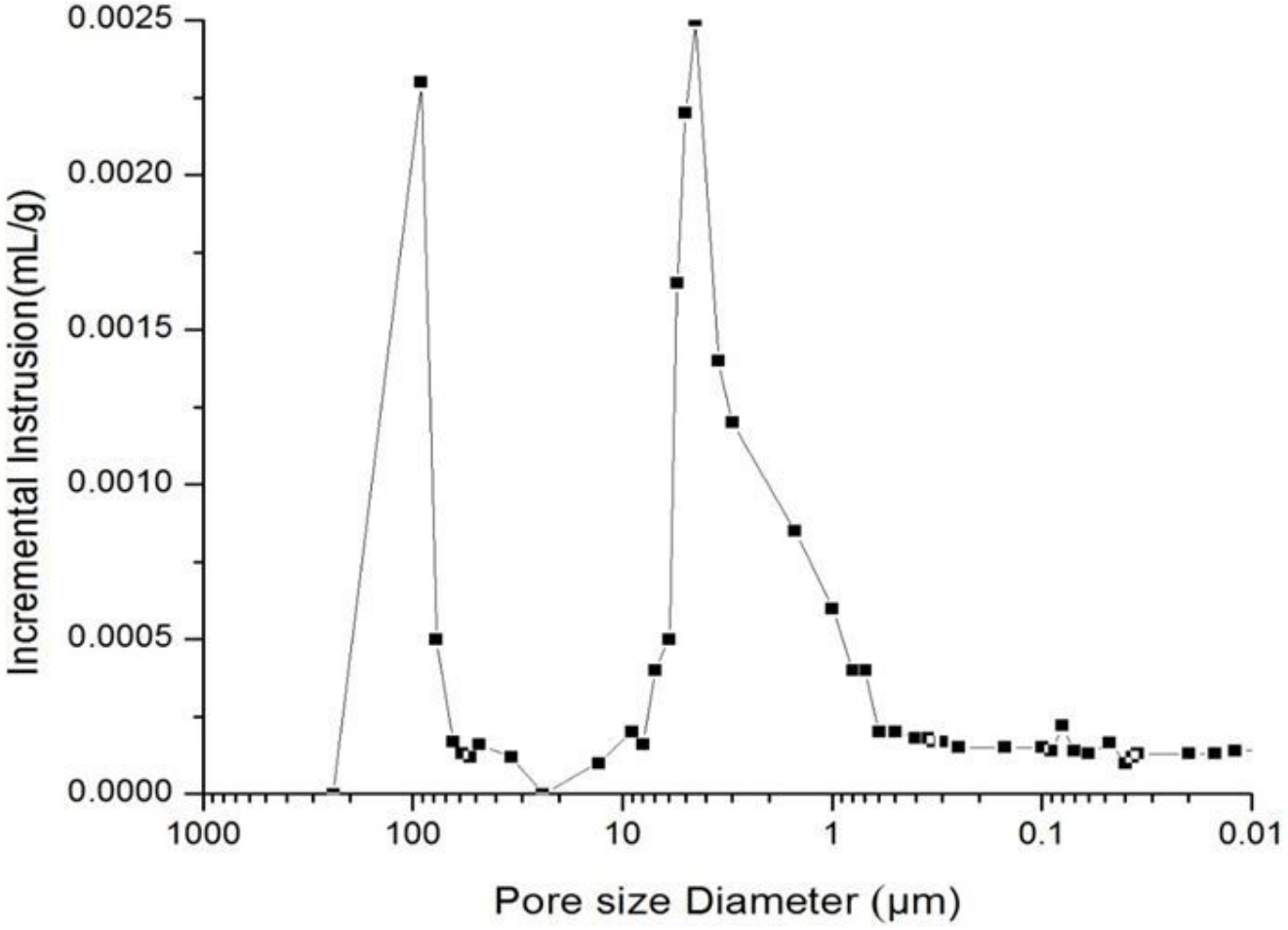

Figure 12

Incremental intrusion of mercury against pore size of batch 1.

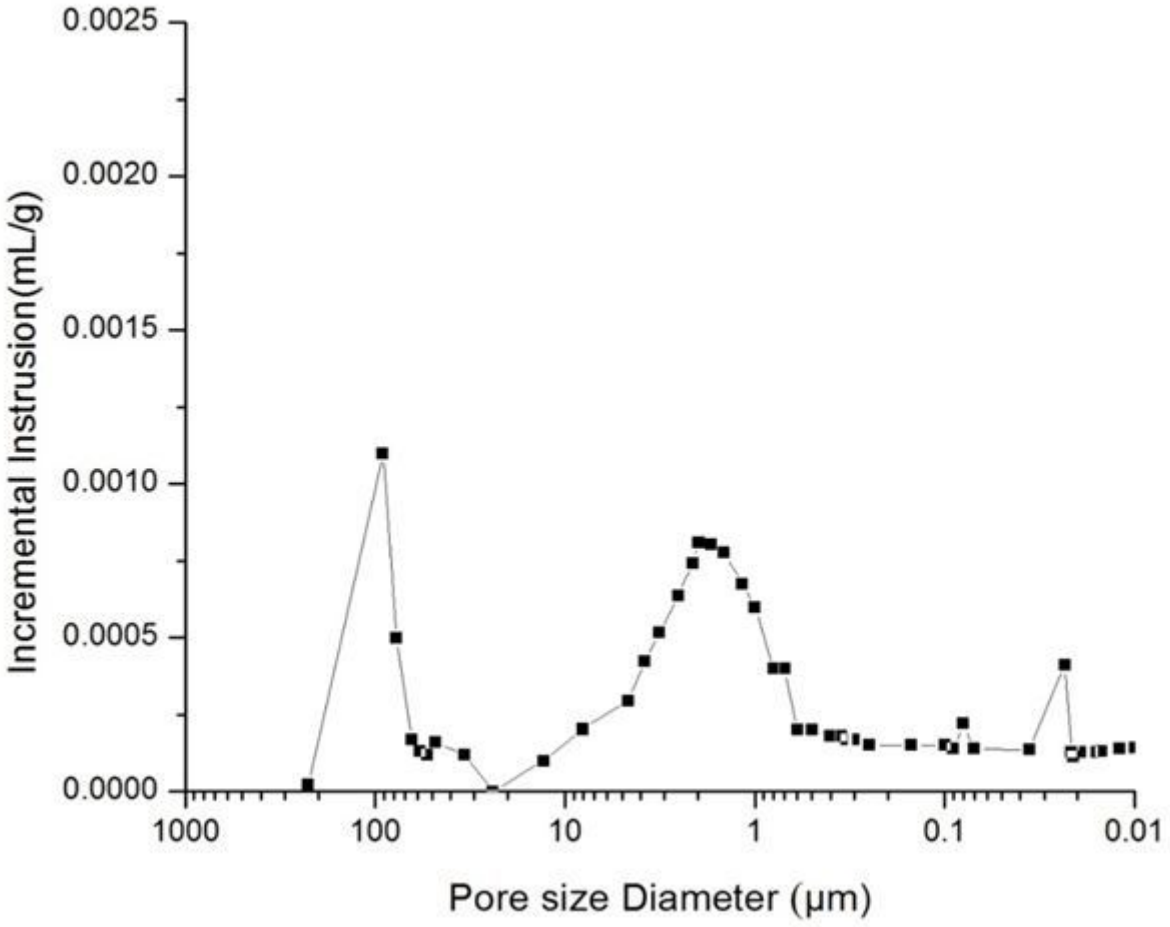

Figure 13

Incremental intrusion of mercury against pore size of batch 3.